# SiO$_2$-Ag$^0$ GENERATION BY SOL-GEL TECHNIQUE FOR ANTIBACTERIAL USE

M. L. OJEDA-MARTÍNEZ[a], I. YAÑEZ-SÁNCHEZ[a], A. ZAMUDIO-OJEDA[b],
F.J. GÁLVEZ-GASTELUM[c], R. MACHUCA-GONZÁLEZ[b],
C. VELÁSQUEZ ORDOÑEZ[a*]

[a]Centro de Investigación en Nanociencia y Nanotecnología Centro Universitario de los Valles, Universidad de Guadalajara, Carretera Guadalajara-Ameca Km 45.5, C.P. 46600, Ameca, Jalisco, México.
[b]Centro Universitario de Ciencias Exactas e Ingenierías, Universidad de Guadalajara, Blvd. Marcelino García Barragán 1421, esq Calzada Olímpica, C.P. 44430, Guadalajara, Jalisco, México.
[c]Unidad de Investigación Cardiovascular, Centro Universitario de Ciencias de la Salud, Universidad de Guadalajara, Sierra Mojada 950, Col. Independencia, C.P. 44340, Guadalajara, Jalisco, México.

Silver nanoparticles (AgNP's) have been immobilized onto silica spheres through the adsorption and subsequent reduction of Ag$^+$ ions on the surface by trisodium citrate. The SiO$_2$-Ag$^0$ spheres were characterized by high resolution transmission electron microscopy (HRTEM), UV-Vis diffuse reflectance (DRS), and Fourier Transform Infrared Spectroscopy (FT-IR). Posterior antibacterial tests of the SiO$_2$-Ag$^0$ spheres were done on *Staphylococcus aureus* (ATCC 6538) and *Escherichia coli* (ATCC 10536); which showed good performance.

## 1. Introduction

Nanotechnology is taking advantage of the manipulation of atoms and molecules, to generate new functional materials and devices that have excellent chemical, physical, and biological properties. The size-induced properties of nanoparticles enable the development of new applications in many areas as microbiology. From the wide range of materials that can be generated, monometallic nanoparticles stand out for their extensive applications in catalysis. Their reduced size increases its surface area, as well as its catalytic activity. [1,2] These investigations are important taking into account that the new antibacterial agents could be used to avoid antibiotic resistance; for example, the *Staphylococcus aureus'* resistance to methicillin demonstrated by Nelson *et al*. [3]

Within this context, nanomaterials have arisen as new promising antimicrobial agents due to their high surface/volume ratio, as well as their unique chemical and physical properties. [4]

The usefulness of Silver (Ag) as an antibacterial agent has been known since ancient times. Catalytic efficiency could be diminished if aggregation occurs between colloidal nanoparticles. It is not always desirable to have these systems in a colloidal form. In order to avoid this, many groups have tried to anchor the nanoparticles on different substrates [5, 6]. For this reason, many silver-based composites are being studied. Many of them are inorganic supports developed for antibacterial Ag-containing materials; for example, zeolite, calcium phosphate, and carbon fiber. Particularly, Ag-supported silica materials are expected to be good candidates for

---

*Corresponding Author: celsovo7@hotmail.com

antibacterial materials due to their fine chemical durability and high antibacterial activity [2]. When Ag is formed on these supporting materials, the release time of Ag can be delayed, generating long term potential [2].

Based on the different wall cellular structures of bacteria, these are classified as Gram-negative or Gram-positive. The structural differences lie in the organization of a key component of the membrane, peptidoglycan. Gram-negative bacteria exhibit only a thin peptidoglycan layer between the cytoplasmic membrane and the outer membrane; in contrast, Gram-positive bacteria lack the outer membrane but have a peptidoglycan layer of about 30 nm thick [7].

In this paper, we report the antibacterial activity of $SiO_2$-$Ag^0$ spheres in two pathogenic bacterial strains, *Escherichia coli* and *Staphylococcus aureus*.

## 2. Experimental section

### 2.1 Synthesis of sphere $SiO_2$-$Ag^0$

Single dispersed colloidal $SiO_2$ particles were prepared by the well know Stöber method [8] which consists in the base-catalyzed hydrolysis of tetraetoxisilane. Aqueous ammonia (5.9 mL of $NH_3$ at 29% in water), ethanol (44.5 mL), and 0.02g $AgNO_3$, were mixed in an Erlenmeyer flash. This solution was placed in water bath at 20°C, after that 1.8 mL of tetraetoxisilane was added and put under intense stirring. In order to assure that the reaction was completed, the solution was gentle stirred during 15 h. Then, 10 mL (11.7 mM) of trisodium citrate ($Na_3C_3H_5O(COO)_3$) were added at 60°C and stirred for 12 hrs. Finally, the solvent was removed from the solution and the product was dried at room temperature.

### 2.2 Characterization techniques
#### 2.2.1 UV-Vis Spectrophotometer
UV-Vis spectra of the sample was acquired in the range 200-900 nm using UV-Vis spectrophotometer Cary 300, equipped with an integrating lab sphere DRA-CA301 DRS, using $BaSO_4$ as the reference.

#### 2.2.2 High Resolution Transmission Electron Microscopy
HRTEM analysis was carried out in a HRTEM TECNAIF 30 electron microscope operating at 300 kV. The samples were prepared by dissolving them in isopropanol. They were then deposited on 300 mesh copper grids and subsequently dried in air before being analyzed by HRTEM.

#### 2.2.3 Fourier Transform Infrared Spectroscopy (FTIR)
The compounds were characterized via FTIR in a Varian 660 Spectrometer. The samples were mixed with potassium bromide and examined directly in their powder state without further preparation.

### 2.3 Antibacterial assay
For antibacterial tests of the $SiO_2$-$Ag^0$ spheres, *Staphylococcus aureus* (ATCC 6538) and *Escherichia coli* (ATCC 10536) strains were selected as models of gram-positive and the gram-negative bacteria, respectively. All plates and materials were sterilized by autoclaving them (vapour, 121°C per 20 minutes) before experiments. The antibacterial activities of $SiO_2$-$Ag^0$ spheres were measured by diffusion assays in 8 mm Luria-Bertani (LB) (Invitrogen ®) plates. The plates were previously seeded with both microorganisms and then $SiO_2$-$Ag^0$ spheres (500 g/mL) were collocated on the media. As our controls $Ag$-$^0$ nanoparticles and ethanol were also placed on plates and incubated at 37°C for 24 h. In the end, the plates were evaluated for the presence or absence of bacterial growth. The zone of inhibition was measured (in milimeters) using a vernier calliper. The experiments were performed by triplicated.

## 3. Results and discussion

### 3.1 UV-Vis Analysis

The absorption peaks due to the surface plasmons resonance (SPR) of the $SiO_2$-$Ag^0$ nanoparticles was in 420 nm (figure 1a). The presence of this peak is consistent with the surface SPR of silver nanoparticles [9, 10]. This is induced by the coupling between the oscillation of the electron cloud on the surface of the Ag nanoparticles and the incident electromagnetic wave in the quasi-static regimen [11]. The silica particles (figure 1b) do not show any characteristic absorption peak in the wavelength range of 200-800 nm.
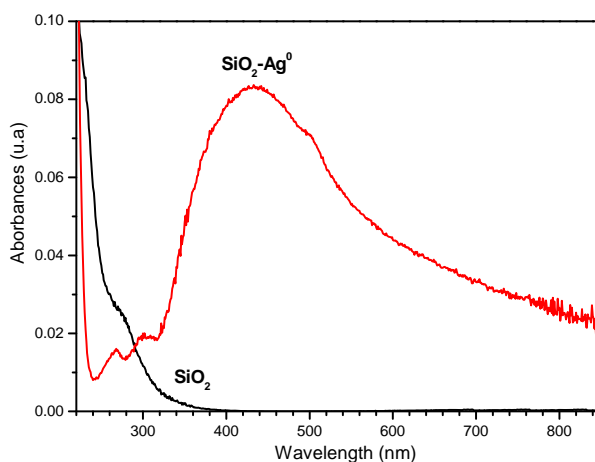


*Fig. 1. The corresponding UV-Vis absorption spectra. $SiO_2$-$Ag^0$ spheres show a plasmon peak at 420 nm (red line), $SiO_2$ spheres (black line).*

### 3.2 FT-IR Analysis

FT-IR transmission spectra of $SiO_2$ and $SiO_2$-$Ag^0$ materials showed bands of molecules associated to the materials (figure 2).

Absorption band spectra corresponding to vibration of the Si-OH bond (960 cm$^{-1}$) [12]. Intensity bands of Si-O-Si bond (at 1095 and 804 cm$^{-1}$ is still present). The band around 480 cm$^{-1}$ shows the strong band associated with Si-O stretching and bending vibrations [13]. At 1150-900 cm$^{-1}$ the bands are related to the symmetric vibration and asymmetric vibration of Si-O-Si, respectively [14]. At 1389 cm$^{-1}$ the band could be attributed to silver particles [15] or to $NO_3^-$ ions from the reaction [16], this is still under discussion.
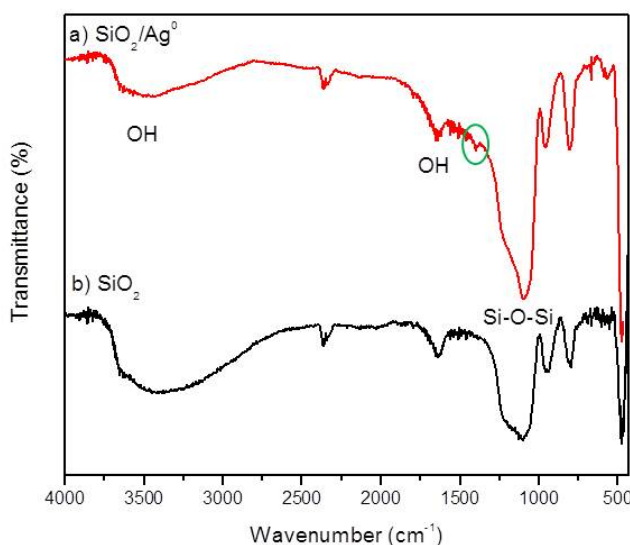


*Fig. 2. FT-IR Red line $SiO_2$-$Ag^0$ sphere, black line $SiO_2$ sphere. The circle indicates the absorption band corresponding to 1389 cm$^{-1}$.*

### 3.3 HRTEM Analysis

Fig. 3a shows HRTEM images of $SiO_2$ spheres embedded with nanometer sized $Ag^0$ particles. In all the samples, $Ag^0$ forms irregular shaped clusters composed by single nanoparticles in the oxide silica matrix. The particles are uniformly arranged on the silica spheres. It is important to note that the stability of the nanoparticles´ size in this kind of matrix shows almost no change.
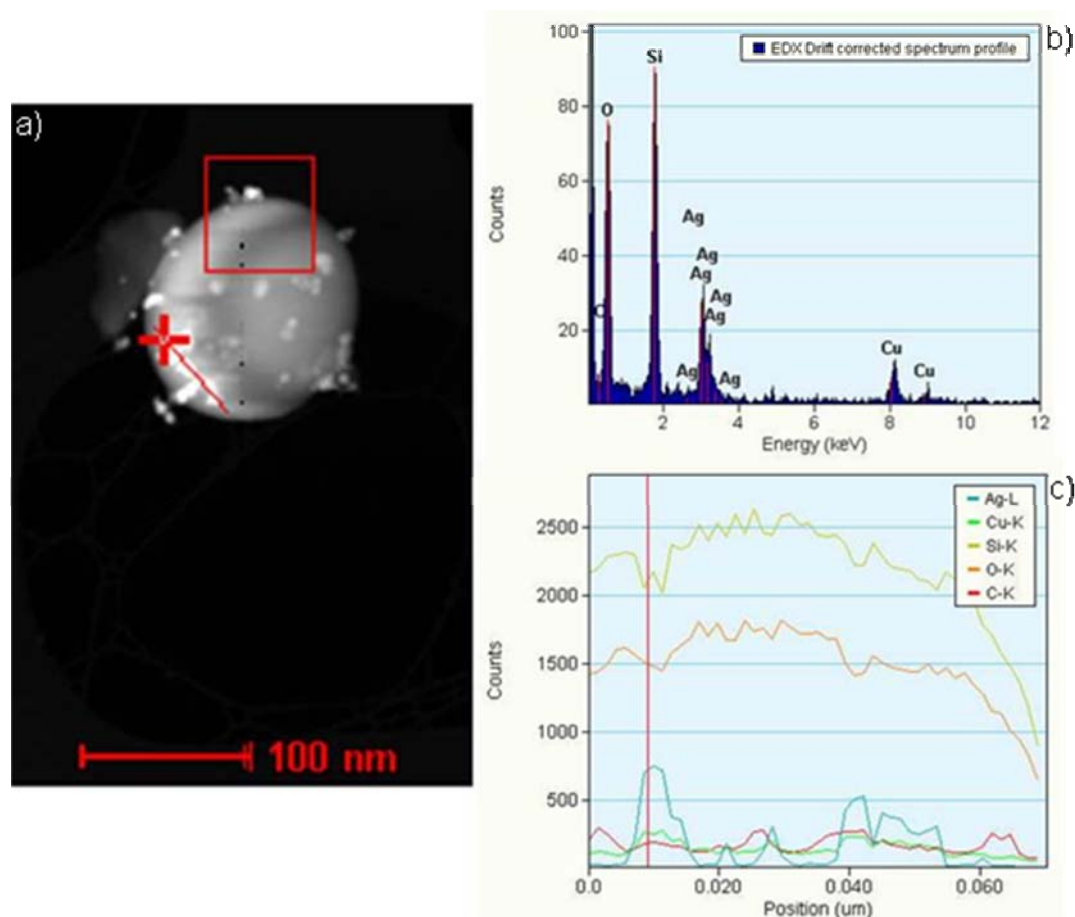


*Fig. 3. HRTEM micrograph image of $SiO_2$-$Ag^0$. (a) STEM image; (b) EDX; (c) Linear mapping, yellow and orange lines (Si and O, respectively), it is understandable to have large amounts $SiO_2$ composition from the matrix; the green line corresponds to $Ag^0$ nanoparticles; red and blue lines correspond to TEM grids (Cu and C).*

Fig. 3b shows chemical analysis by energy-dispersive spectroscopy (EDS) of both matrix and nanoparticles. This confirms the existence of silver nanoparticles in the silica. This study indicates the presence of different materials on the support, obtained from the chemical composition of the $SiO_2$-$Ag^0$ sphere. The Cu and C signals come from the carbon-coated copper grids.

Fig. 3c shows a linear mapping analysis with five different colour lines, each one corresponds to different chemical elements. The green line corresponds to $Ag^0$ which shows peaks and valleys, indicating presence and absence of silver nanoparticles on the sphere´s surface.

### 3.4 Antibacterial Activity

The antibacterial activity was tested against two pathogenic bacteria strains, *Staphylococcus aureus* and *Escherichia coli*. The maximum zone of inhibition was found in the group of $SiO_2$-$Ag^0$ spheres (~26 mm diameter in both strains) in comparison to $Ag^0$ nanoparticles (~17 mm diameter in both strains), as shown in figure 4. However, the best antibacterial effect of $SiO_2$-$Ag^0$ spheres was presented in the *E. coli* (2.73 cm) against *S. aureus* (2.36 cm). The treatment

with $Ag^0$ nanoparticles was different in both strains (1.3 and 1.12 cm, respectively) but with less effect in growth inhibition. Our study indicated similar results to those reported by Young H, *et al*., who mentions that this difference in the antibacterial effect may be partially explained by the fact that $Ag^0$ nanoparticles formed on the surface of $SiO_2$ carry the opposite charge with Gram-negative bacteria (*E. coli),* thereby killing them more easily than Gram–positive bacteria (*S. aureus)* due to the electrostatic attraction **[2]**.

Other reasoning is exposed by Young H, *et al*, where the aggregation of $Ag^0$ nanoparticles causes deterioration of the antibacterial activity. This indicates that the activity would greatly improve with increased amounts of $Ag^0$ nanoparticles, formed on the surface of $SiO_2$ spheres, due to better uniformity on the surface of the spheres and without huge aggregations of nanoparticles as in colloidal $Ag^0$ **[2]**.

In respect to antibacterial mechanism, Feng *et al*. reported a mechanistic study of the antibacterial effect of silver ions on *E. coli* and *S. aureus* and postulated that as a reaction against the denaturation effects of silver ions, DNA molecules become condensed and lose their replication abilities. He also says that silver ions interact with thiol groups in proteins, which induces the inactivation of bacterial proteins **[17]**. In addition, several authors have suggested that these nanoparticles can penetrate inside the bacteria causing cell damage by interaction with sulphur and phosphorus compounds, like DNA **[18]**. Morones J. *et al*., showed results that indicate that the bactericidal properties of the nanoparticles are size dependent, since the only nanoparticles that present direct interaction with the bacteria preferentially have a diameter of ~1–10 nm **[19]**. Pal *et al*., reported in a comparative study, using $Ag^0$ nanoparticles of different shape and their resulting bactericidal properties, which demonstrates that silver nanoparticles undergo a shape-dependent interaction with the gram-negative organism *E.coli* **[20]**.

Finally, in an article published by Anas A, *et al*., it is demonstrated that $SiO_2$-$Ag^0$ nanocomposites invade the cytoplasm of multiple drug-resistant bacteria, as *Pseudomona aeruginosa* (gram-negative bacteria), by impinging upon the cell wall integrity and killing the cell by interfering with electron transport chains and its genetic stability **[21]**.
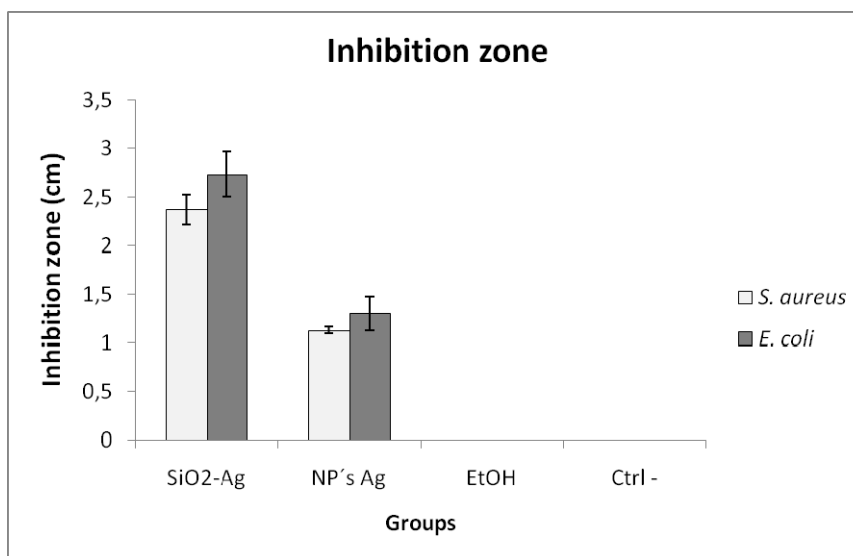


*Fig. 4. Effects of $SiO_2$-$Ag^0$, zone of inhibition was expressed in cm.*

## 4. Conclusions

The assembly of Ag nanoparticles with $SiO_2$ sphere enable certain degree of control when it comes to the physical and chemical properties of Ag nanoparticles. The antimicrobial assay showed that $SiO_2$-$Ag^0$ presented good antibacterial performance. The explanation that we propose as a possible mechanism of the $SiO_2$-$Ag^0$ spheres in the system by which it exhibits a better activity than $Ag^0$ nanoparticles colloids, is due to gradual ionization of silver increasing their

414

antibacterial properties. In addition, Ag nanoparticles are uniformly distributed around silica matrix, which increases their surface to area ratio of exposure.

## References

[1] N. Toshima, Y. Wang, Langmuir **10**, 4574 (1994).
[2] Y.H. Kim, D.K. Lee, H.G. Cha, C.W. Kim, Y.S. Kang, J. Phys. Chem. **111**, 3629 (2007).
[3] N. Durán, P.D. Marcato, G.I. De Souza, O.L. Alves, E. Esposito, J. Biomed. Nanotechnol. **3**, 203 (2007).
[4] V. Dal Lago, M. B. Cardoso, L. Franca de Oliveira, Centro nacional de pesquisa em energia e materiais, 2011, Brasil.
[5] L. Bois., F. Bessueille, F. Chassagneux. Y. Balttie, N. Destouches. C. Hobert, A. Boukenter, S. Parola, Colloid and Surface A. Physicochem. Eng. Aspects **325**, 86 (2008).
[6] M. L. Viger, L. S. Live, O. D. Therrien, D. Boudreau Plasmonic **3,** 33 (2008).
[7] J. R. Morones, J.L. Elechiguerra, A. Camacho, K. Holt, J.B. Kouri, J.T. Ramírez, M.J. Yacaman, Nanotechnology **16,** 2346 (2005).
[8] W. Stöber, A. Fink, E. Bohn, J. Colloids Interface Sci. **26**, 62 (1968).
[9] S. Ayyappan, R. Srinivasa-Gopalan, G. N. Subbanna, C. N. R. Rao, J. Mater. Res. **12,** (1997).
[10] T. Ung, L. M. Liz-Marzán, P. Mulvaney, Langmuir **14**, 3740 (1998).
[11] U. Kreibig, M. Vollmer, Optical properties of metal cluster, Springer, New York (1999).
[12] L. X. Zhang, J. L. Shi, J. Yu, Z. L. Hua, X. G. Zhao, M. L. Ruan, Adv. Mater. **14**, 1510 (2002).
[13] W. H. Green, K. P. Le, J. Grey, T. T. Au, M. J. Sailor, Science **276**, (1997).
[14] L. L. Hench, Chem. Rev. **90**, 33 (1990).
[15] G. Gnanakumar, B. Karunagaran, K. S. Nahm, R. N. Elizabeth, Nanoscale Res. Lett. **4**, 452 (2009).
[16] H. J Jeon, S. C. Yi, S. G. Oh, Biomaterials **24**, 4921 (2003).
[17] Q. L. Feng, J. Wu, G. Q. Chen, F. Z. Cui, T. M. Kim, J. O. Kim, J. Biomed. Mater. Res. **52**, 662 (2000).
[18] A. Panácek, L. Kvítek, R. Prucek, M. Kolár, R. Vecerová, N. Pizúrová, V. K. Sharma, T. Nevecná, R. Zboril, J. Phys. Chem. B. **110**, 16248 (2006).
[19] J.R. Morones, J.L. Elechiguerra, A. Camacho, K. Holt, J. B. Kouri, J. T. Ramírez, M. J. Yacaman, Nanotechnology **16**, 2346 (2005).
[20] S. Pal, Y. K. Tak, J. M. Song, App. Env. Microb. **73**, 1712 (2007).
[21] A. Anas, J. Jiya, M. J. Rameez, P. B. Anand, M. R. Anantharaman, S. Nair, Lett. Appl. Microbiol. in press (2012).